Study of the relationship between non-dimensional roughness length and wave age, effected by wave directionality

Naoya Suzuki[1], Naoto Ebuchi[2], Chaofang Zhao[1,3], Isao Watabe[4] and Yasuhiro Sugimori[1]

[1] *Center for Environmental Remote Sensing (CEReS), Chiba University, 1-33 Yayoi Inage Chiba, 263-8522 Japan.*

[2] *Center for Atmospheric and Oceanic Studies, Graduate School of Science, Tohoku University, Aoba, Sendai 980-8578, Japan.*

[3] *Ocean Remote Sensing Laboratory, Ocean University of Qingdao, China.*

[4] *National Research Institute for Earth Science and Disaster Prevention, Science and Technology Agency, 9-2 Nijigahama, Hiratsuka, Kanagawa, 254-0823 Japan.*

Relationship between the non-dimensional roughness length and inverse of wave age has been discussed without consideration of wave directions, though wind wave field consists of various directional component waves. In this study we observe wave heights by an array of four wave gauges at the Hiratsuka Tower of (Independent Administrative Institution) National Research Institute for Earth Science and Disaster Prevention (NIED), Japan, and discuss the effect of wave directionality. As a result, the data sets were classified into two different groups according to the directional wave spectrum distribution. In case 1 only swell and wind waves exist and in case 2 there exist wave components from several directions. It is shown that the case of multiple-directional component waves (case 2) may affect the non-dimensional roughness length and friction velocity.

1. Introduction

The sea surface wind stress has generally been estimated using the drag coefficient C_D. Many efforts have recently been made to elucidate the wave dependence of the sea-surface roughness parameter z_0, which has one-to-one correspondence to C_D under near-neutral conditions. However, there still exists considerable disagreement among investigators for the parameterization of the coefficient, especially for its dependence on wave growth.

In order to estimate the wind stress and roughness length, Charnock's (1955) well known formula,

$$\frac{gz_0}{u_*^2} = \beta, \tag{1}$$

has widely been utilized, where g is the acceleration of gravity, and β is a constant. For the value of β, there seems to be considerable disagreement among authors. For example, Charnock (1955) proposed 0.0068, Smith and Banke (1975) gave 0.0130, Garrat (1977) suggested 0.0144, and Wu (1980) proposed 0.0185. A possible reason for the disagreement might be poor quality and quantity of wind stress measurements. Also effects of waves on the wind stress should be considered explicitly.

Stewart (1974) presented a general form for the wave dependence of the wind stress as a function of wave age,

$$\frac{gz_0}{u_*^2} = f\left[\frac{C_P}{u_*}\right], \tag{2}$$

where C_P is the phase speed of wind waves of the spectral peak frequency. By assuming the lin-

Keywords. Wind wave; roughness length; wave age.

Proc. Indian Acad. Sci. (Earth Planet. Sci.), **111**, No. 3, September 2002, pp. 305–313

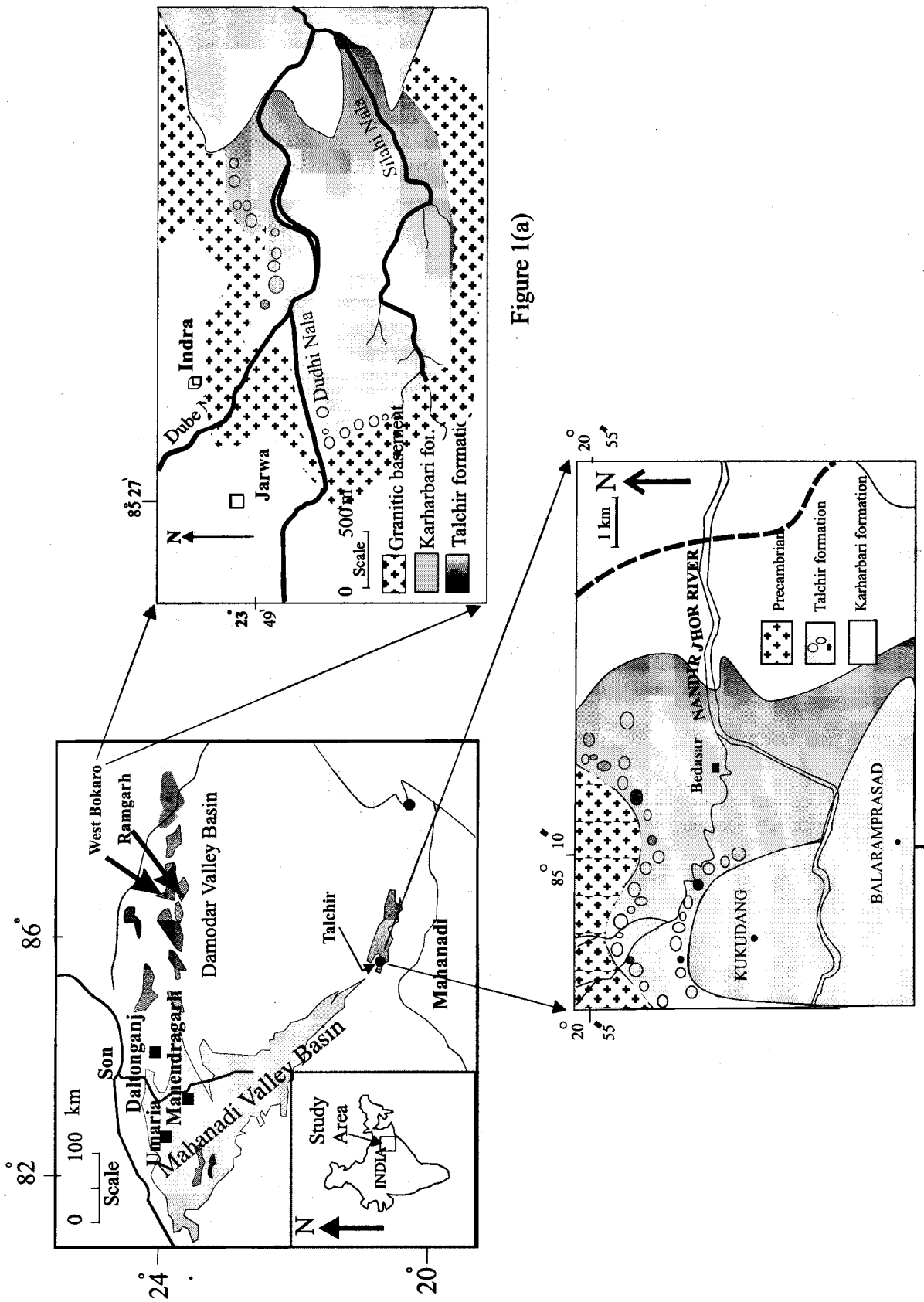

Figure 1. Three major Gondwana basins of peninsular India. Present work is confined to Damodar valley basin (west Bokaro and Ramgarh sub-basins) and Mahanadi valley basin (Talchir sub-basin). (**a**): Geological map of west Bokaro sub-basin. (**b**): Geological map of Talchir basin showing Nandirjhor Nala section.

obtained by comparing γ-ray intensities of the samples with those of reference standard rocks, JB-1 (supplied by Japan Geological Survey) and BCR-1, which were irradiated with the nodule samples. The Allende meteorite reference sample prepared by the Smithsonian Institute, USA also was simultaneously irradiated. Analytical errors due to counting statistics are less than 5% (less than 2% for most elements).

3. Results and discussions

3.1 *Sedimentation in a fresh water lake*

Before discussing the elemental data it is worthwhile to summarize the conclusions based on the stable isotope analysis of the nodules reported in our recent work (Bhattacharya *et al* 2001). An important feature of the stable isotope data is highly depleted oxygen isotopic composition (mean -19.5‰ w.r.t PDB) of a majority of the nodules. This suggests that precipitation of the Talchir carbonates took place in a fresh water environment because marine carbonate cements are characterized by δ^{18}O values close to zero or slightly negative (Veizer *et al* 1999). This conclusion is also supported by the depleted carbon isotope ratio of the nodules (mean -9.7‰ w.r.t. PDB) indicating mixing of biogenic carbon with normal sedimentary carbon in making up the bicarbonate reservoir of the basin. The carbon isotope ratio in ancient sedimentary carbonates is least affected during diagenesis and alteration (Schidlowski and Aharon 1992). Therefore, the observed δ^{13}C values of the nodules strongly indicate that the basin was made up of fresh water (if the precipitation took place in sea water the carbon isotope ratio would have been within ± 2‰).

As mentioned before, petrographic investigations of the nodular carbonates indicate that most of the nodules represent *in situ* primary precipitates. Cathodoluminescence observations suggest that a majority of the calcites were precipitated from water having high Mn/Fe ratio, as expected in glacio-fluvial condition and contrary to that expected if the Talchir carbonates were formed in a marine regime with low Mn/Fe ratio (Tobin *et al* 1999). Moreover, the association of the nodules with glacial diamictites suggests freshwater lakes formed by glacier melt-water as probable milieu for sedimentation and carbonate precipitation (schematically shown in figure 2). The nodules probably formed inside the sediment bed by radial growth around a favourable starting nucleous induced by physico-chemical conditions of the micro-environment. The growth process involves compaction of the detrital minerals by cementation

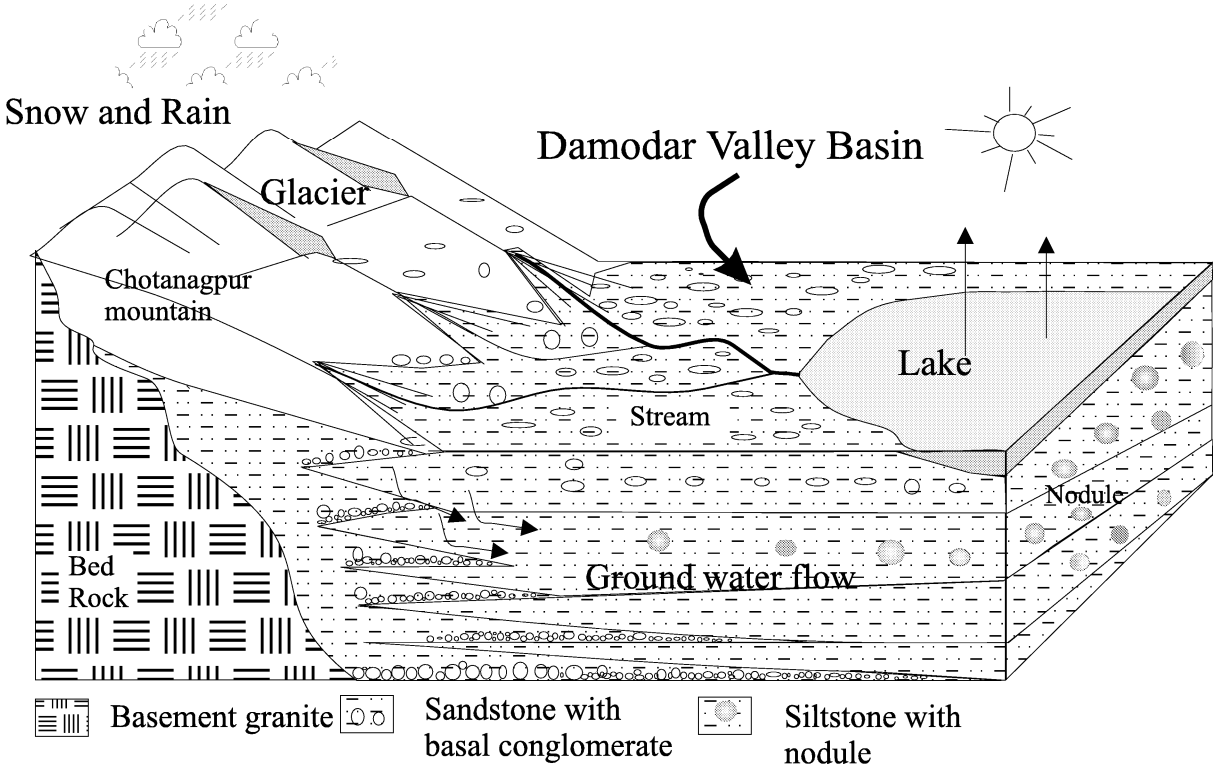

Figure 2. Schematic diagram showing the proposed environment of nodule formation based on the stable isotope analyses of carbonate phase (Bhattacharya *et al* 2001). The Chotanagpur mountain is shown as host for the glaciers draining into Damodar valley basin based on the present geochemical analysis.

Table 1. *Salient features of retrieval algorithms.*

Features		MSMR algorithm	Wentz algorithm
1. Type		Statistical technique using Radiative Transfer Simulations (Gohil *et al* 2000)	Minimization approach between measured and simulated brightness temperatures (Wentz, 1997).
2. Channels for-			
	IWV	18V, 18H, 21V, 21H	V22, V37, H37
	WS	6V,6H,10V,10H,18V,18H,21V,21H 10V,10H,18V,18H,21V,21H	V22, V37, H37
	CLW	18V,18H,21V,21H	V22, V37, H37
	SST	6V,6H,10V,10H,18V,18H,21V,21H	
3. Other inputs in retrieval algorithms		Climate SST and incidence angle	Average SST and incidence angle

satellites is essential. Ali (2000) has presented a comprehensive comparison of all GPDs (except CLW) with *in situ* and analysed fields, and found reasonably good agreement. Varma *et al* (1999) have compared scan mode MSMR derived CLW, IWV and OWS with similar products from SSM/I over the Indian Ocean region. The present study is aimed at inter-comparison of MSMR derived gridded products (except SST) with similar products from SSM/I and TMI over the global oceans.

The difference in MSMR GPDs with respect to SSM/I and TMI are due to the difference in their frequencies at which measurements are made, noise figures and algorithm. The basic features of retrieval algorithm for SSM/I and TMI, and MSMR are shown in table 1, which shows the difference in the basic approach as well as the channels used.

2. Instruments and data

2.1 *IRS-P4 MSMR data*

MSMR on board IRS-P4 (Oceansat-I) provides measurement of brightness temperatures (Tbs) at 6.6, 10, 18 and 21 GHz frequencies in both horizontal and vertical polarisations. IRS-P4 is in a sun synchronous orbit with ascent at equator at 2340 hr and descent at 1140 hr local time. The four operational products available from MSMR are Cloud Liquid Water (CLW), Integrated Water Vapour (IWV), Ocean Surface Wind Speed (OWS) and Sea Surface Temperature (SST). MSMR products are generated in three resolution grids of 150, 75 and 50 kms, respectively. Derivation of CLW and IWV use only high frequency channels, and they are available in all three grids. OWS is available in two grids of 150 and 75 km, with the use of all 8 channels in 150 km grid, and use of 6 channels in 75 km grid (without 6 GHz). Derivation of SST uses all 8 channels and thus is available only in 150 km grid. Table 2 shows the theoretical accuracy of MSMR products.

Table 2. *Theoretical retrieval accuracy of MSMR GPDs.*

Parameter	Tropic	Midlat	Polar
SST (K) (grid 1)	1.52	1.92	1.90
OWS (ms^{-1}) (grid 1)	1.63	1.59	1.51
OWS (ms^{-1}) (grid 2)	2.10	2.00	1.91
IWV ($g\ cm^{-2}$)' (grids 1,2, 3)	0.20	0.18	0.15
CLW ($mg\ cm^{-2}$) (grids 1, 2, 3)	13.0	11.0	9.0

MSMR geophysical data are available daywise (24 hrs) in three grids as mentioned above, with data quality flag.

2.2 *SSM/I and TMI data*

SSM/I is a four frequency, seven channel radiometer. The SSM/I is operated at 19.35, 22.235, 37.0 and 85.5 GHz frequencies. TMI frequencies are almost similar to SSM/I except for additional 10.7 GHz frequency and a 21.3 GHz frequency instead of 22.235 GHz for SSM/I. TMI and SSM/I operate in dual polarizations, V and H, except 22.235 GHz that operates only in V polarization. Three satellites which carry onboard SSM/I, namely F11, F13 and F14, are presently operational in sun-synchronous orbit with equator ascending time at 1925, 1754 and 2046 LST, respectively. On the other hand, TMI onboard TRMM (Tropical Rainfall Measuring Mission) satellite is in a low altitude (218 miles), low inclination, and non-sun-synchronous orbit.

The SSM/I -F13 and -F14 global swath mode data are provided by Global Hydrology Resource Centre (GHRC) of NOAA/USA. The data are available with footprint sampling resolution of 25 km for 19, 22 and 37 GHz channels (called low